Rheo-optical studies on the deformation mechanism of semicrystalline polymers: 7. Analyses of orientational and form birefringence of tubular-extruded poly(butene-1) films

Akira Todo*, Takeji Hashimoto, Yasuhisa Tsukahara and Hiromichi Kawai
Department of Polymer Chemistry, Faculty of Engineering, Kyoto University, Kyoto 606, Japan

Birefringence studies have been carried out to assess amorphous chain orientation of the 'row-nucleated' superstructure developed by crystallization from oriented melts. Birefringence, measured as a function of percentage elongation of film specimens subjected to stretching along the extrusion direction (the films are prepared by a tubular extrusion) and as a function of the refractive indices of the immersion liquid was separated into orientational and form birefringences. The orientational birefringence was further separated into the birefringence arising from crystal orientation and that from the amorphous chain orientation, utilizing orientation measurements made on crystals by wide-angle X-ray diffraction; the results indicate that the two contributions are comparable for a particular value of the intrinsic birefringence of the crystal $\Delta_c^o = 0.0108$, and the contribution of the amorphous tie chains is substantial. The form birefringence contributes negatively to the total birefringence and the negative contribution increases with increasing percentage elongation owing to the special morphology of the stacked lamellae and the decrease of interlamellar density with stretching. Its contribution to the total birefringence is initially minor (~6%) but increases with elongation until most of the total birefringence arises from the form birefringence. The form birefringence calculated using Franklin's theory shows a relatively good agreement with the experimental values, indicating that the deformation model involving a uniform interlamellar lowering of density is appropriate.

INTRODUCTION

In the preceding paper (Part 6[1]) we reported the deformation mechanism and recoverability of the 'row-nucleated' sheaf-like structure developed in tubular extruded films of poly(butene-1) at sub-microscopic and microscopic structure levels. It was clarified in the paper that the mechanical properties are strongly dependent upon the nature of the amorphous phase and its deformation behaviour.

For example, the films exhibit springy properties[2,3] only at temperatures above the glass transition, while the typical springy materials such as Celcon fibres[2-4] exhibit these properties even below the glass transition temperatures. The negative temperature coefficient of the retractive force of the poly(butene-1) films has been shown to be two orders of magnitude smaller than the springy Celcon fibres. These differences are proposed to be associated with the difference in the nature of the amorphous phase and its deformation behaviour[1].

In this article we will attempt to assess amorphous chain orientation for the as-prepared films and for films stretched along the extrusion direction (*ED*) by conducting birefringence studies. It is one of our objectives in this study to separate birefringence associated with the amorphous chain orientation from that due to crystal orientation and form birefringence[5]. The estimated birefringence due to amorphous chain orientation may be further analysed to gain some insights on the deformation and orientation of amorphous phase which is composed of tie chains, loops, cilia and floating chains, based upon an approach as proposed by Stein *et al.*[6] and Gaylord *et al.*[7]. We aim to accomplish such analyses as well as the analysis of their contributions to the retractive force and modulus[8], though this article deals with only a part of the work.

As discussed in the preceding paper (Part 6)[1], when specimens are stretched along the *ED*, the interlamellar amorphous layer thickens, leading to a lowering of density of the amorphous phase and thus creating a bigger difference in refractive index between the crystalline and amorphous phase. Due to the special morphology and deformation behaviour, the film specimens uniformly whiten and exhibit extraordinarily large form birefringence. The separation of the form birefringence and analysis based upon the theories of Wiener[5] or Franklin[9] is another important objective of this work.

EXPERIMENTAL

The morphology and deformation mechanism of tubular extruded poly(butene-1) films used in this work were fully

* Present address: The Research Center, Mitsui Petrochemical Industries Ltd, Waki-cho, Kuga-gun, Yamaguchi-ken, Japan

0032-3861/79/080943-08$02.00

Table 1 Immersion liquids used for birefringence measurements

Solvent	Refractive index n_D (25°C)	Solvent	Refractive index n_D (25°C)
Methanol	1.326	1,2,3-Trichlorobenzene	1.567
Ethanol	1.359	*o*-Toluidine	1.570
n-Hexane	1.372	Mixture of cedar oil and bromonaphthalene	1.589
Chloroform	1.444		1.617
Benzene	1.498		1.622
Chlorobenzene	1.523		1.651
1,2-Dibromoethane	1.538	Bromonapthalene	1.662
o-Dichlorobenzene	1.551		

discussed in a previous paper[1]. A brief summary is described below. The film specimens had weight-average crystallinities of 60–65% and showed springy properties only at temperatures above the glass transition. The internal structure is composed of an oriented sheaf-like crystalline superstructure [a diverging sheaf of crystal lamellae oriented normal to the extrusion direction (*ED*)], the centre of which is aligned nearly parallel to the *ED*. The superstructure results from overgrowth of lamellae from rows of nucleating points which are oriented nearly parallel to the *ED*. The overgrowth occurs initially in a direction normal to the *ED*. In the course of growth, the fronts occasionally branch at some distance and angle into new lamellae giving rise to the diverging sheaf of lamellae.

When the specimens are stretched along the *ED*, the sheaf undergoes an affine deformation with the bulk strain resulting in orientation of the lamellar axes toward the *ED*, thus splaying apart the interlamellar spacings, and lowering the density of the interlamellar amorphous region. The density lowering of the interlamellar amorphous region was experimentally verified by changes in the relative intensity of the small-angle X-ray scattering maxima with stretching[1]. Such deformation of the lamellar networks, i.e. stacks of lamellae connected by tie links or tie chains as discussed in detail in the preceding paper is responsible for the change in measured birefringence with bulk elongation.

It is important to note that the extensions of the interlamellar spacings are uniform and identical to those of the bulk specimens for the following analyses of the molecular birefringence and also for understanding the long range elasticity of the films. The orientation of the lamellae involves a change in the second-order orientation factor of the crystal *c*-axis

$$f_c = [3 < \cos^2\theta_c > - 1]/2$$

where θ_c is the angle between the crystal *c*-axis and the stretching direction, and therefore a change in:

$$\Delta_{cr} = \phi_c f_c \Delta_c^0$$

Δ_c^0 and ϕ_c being the intrinsic birefringence of the crystal and the volume average crystallinity, respectively, i.e. the birefringence arising from the crystal orientation. The extension of the interlamellar spacing and the lamellar orientation also involve changes in ϕ_c, f_{am} (the second order orientation factor of the amorphous chain segments) and thus of $\Delta_{am} = (1 - \phi_c) f_{am} \Delta^0_{amc}$, Δ^0_{amc} – the intrinsic birefringence of the amorphous chain. The deformation also changes the form birefringence Δ_{form}, i.e. the birefringence arising from the distortion of the electric field of the incident light wave at the phase boundaries of crystalline and amorphous phases.

Thus the molecular orientation in the amorphous region and its variation upon stretching the specimens along the *ED* can be evaluated in terms of the amorphous birefringence Δ_{am} by separating Δ_{cr} and Δ_{form} from the measured total birefringence Δn:

$$\Delta n = \Delta_{cr} + \Delta_{am} + \Delta_{form}$$

$$\Delta_{cr} = \phi_c f_c \Delta_c^0, \qquad \Delta_{am} = (1 - \phi_c) f_{am} \Delta^0_{amc} \qquad (1)$$

For this purpose the birefringence Δn was measured for the specimens stretched and then immersed in liquids as a function of the extension ratios of the specimens (λ) and the refractive indices n_s of the immersion liquids. The specimens stretched along the *ED* and held at constant length were immersed in the liquids for 48 h prior to the birefringence measurements with a Berek compensator. The liquids used are shown in *Table 1* and are relatively inert to the specimens, the degree of swelling being less than 12%.

THEORETICAL

Cvikl, Moroi, and Franklin[9] developed a theory of the form birefringence for a system composed of an unlimited number of alternating lamellae of arbitrary anisotropic homogeneous materials. The theory is a generalized form of that developed by Wiener[5] in that it takes into account an optical anisotropy of each phase. For the special case of optically isotropic two-phase systems with sharp phase boundaries, the result reduces to Wiener's equation.

Consider an oriented assembly composed of alternating crystal and amorphous layers with sharp phase boundaries oriented normal to assembly axis (*Figure 1*). For a special case where each phase has uniaxially symmetric optical aniso-

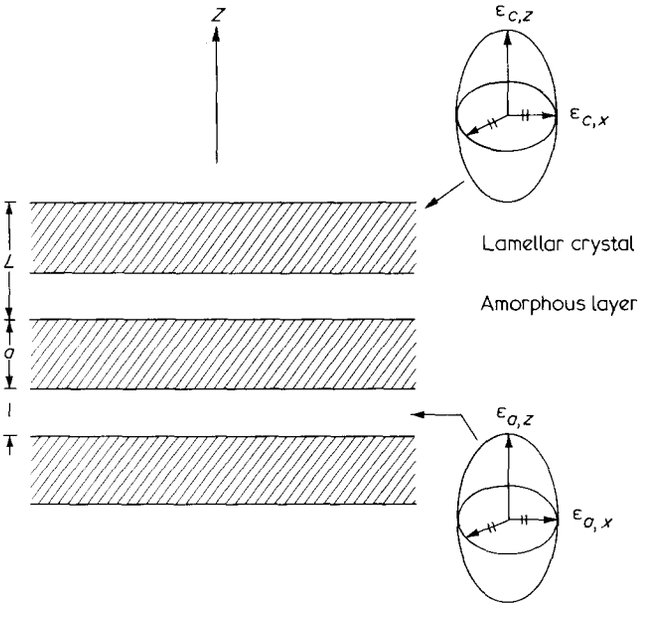

Figure 1 One-dimensional assembly of alternating crystalline (lamellar) and amorphous layers of thickness *a* and *l* and long identity period *L*. The lamellar and amorphous layers are assumed to have uniaxial optical anisotropy with their optical axes being parallel to the assembly axis *Z*.

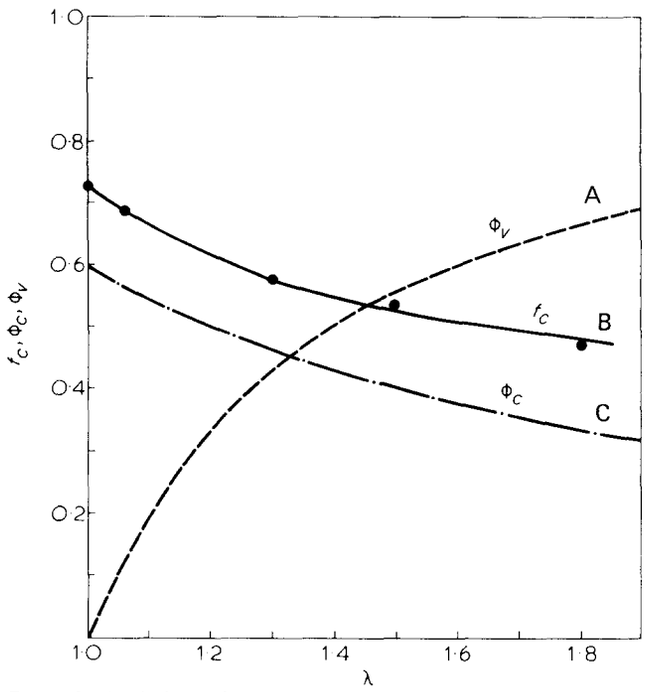

Figure 2 Variations of the crystal *c*-axis orientation factor f_c, volume average crystallinity ϕ_c, and the parameter ϕ_v related to expansion of the amorphous layer thickness with extension ratios λ of the bulk specimen. A, ϕ_v; B, f_c; C, ϕ_c

tropy with dielectric tensors $\underset{\sim}{\epsilon}_c$ and $\underset{\sim}{\epsilon}_a$ and its principal optical axis has the same orientation, parallel to the assembly axis z:

$$\underset{\sim}{\epsilon}_c = \begin{pmatrix} \epsilon_{c,x} & 0 & 0 \\ 0 & \epsilon_{c,x} & 0 \\ 0 & 0 & \epsilon_{c,z} \end{pmatrix} \tag{2}$$

$$\underset{\sim}{\epsilon}_a = \begin{pmatrix} \epsilon_{a,x} & 0 & 0 \\ 0 & \epsilon_{a,x} & 0 \\ 0 & 0 & \epsilon_{a,z} \end{pmatrix}$$

the dielectric tensor of the assembly ϵ is given by:

$$\underset{\sim}{\epsilon} = \begin{pmatrix} \epsilon_x & 0 & 0 \\ 0 & \epsilon_y & 0 \\ 0 & 0 & \epsilon_z \end{pmatrix} \tag{3}$$

where

$$\epsilon_x = \epsilon_y = \phi_c \epsilon_{c,x} + \phi_a \epsilon_{a,x} \tag{4}$$

$$\epsilon_z = (\phi_c/\epsilon_{c,z} + \phi_a/\epsilon_{a,z})^{-1} \tag{5}$$

ϕ_c and ϕ_a are the volume fractions of crystal and amorphous layers, respectively. The equations are derived using the assumption of the long wavelength limit where the long identity period L is small compared with the wavelength of the incident light beam. The assumption is legitimate in our case, since L is of the order of 100Å.

The birefringence of the assembly, Δ_{assembly}, and of crystal and amorphous layers, Δ_c^0 and Δ_{amp}^0 in the assembly are given by:

$$\Delta_{\text{assembly}} = n_z - n_x = \epsilon_z^{1/2} - \epsilon_x^{1/2}$$

$$\Delta_c^0 = n_{c,z} - n_{c,x} = \epsilon_{c,z}^{1/2} - \epsilon_{c,x}^{1/2}$$

$$\Delta_{\text{amp}}^0 = n_{a,z} - n_{a,x} = \epsilon_{a,z}^{1/2} - \epsilon_{a,x}^{1/2} \tag{6}$$

where n values are the refractive indices corresponding to ϵ_s. An apparent form birefringence Δ_{form}^0 of the assembly may be defined as:

$$\Delta_{\text{form}}^0 \equiv \Delta_{\text{assembly}} - (\phi_c \Delta_c^0 + \phi_a \Delta_{\text{amp}}^0) \tag{7}$$

It should be noted that equations (4) and (5) are derived for the sharp boundaries. The theory can be also applied even to the case of the diffuse boundaries. However, the effect turns out to be negligibly small in the case where the volume fraction of the diffuse phase boundaries is of the order of 0.1 (ref 10). Most of the crystalline polymers have about this fraction of the phase boundaries[11].

MODEL AND PRINCIPLE

In this section we will discuss the model and methods to evaluate unknown parameters in equations (4) and (5) and to separate each contribution from the total birefringence.

In the previous section the assembly z-axis is assumed to have perfect orientation. In the case where the z-axis has a uniaxially symmetric orientation distribution with respect to a reference axis (i.e. extrusion direction) as reported in the previous work[1], the observed birefringence from the system is given by:

$$\Delta n = \Delta_{\text{assembly}} f_z \tag{8}$$

where f_z is the second-order orientation factor of the assembly axis with respect to the stretching direction. In this analysis we assume that:

$$f_z \simeq f_c \tag{9}$$

The assumption is legitimate to good accuracy because the degree of lamellar twisting around the axis has been found to be small from the previous study and the chain axes orient nearly parallel to the lamellar normals.

When the specimen is stretched along the *ED*, Δn changes because f_z (or f_c) and Δ_{assembly} are a function of λ, bulk elongation ratio, or elongation ratio of the lamellar spacing, L/L_0 (L_0, L being the lamellar spacings for unstretched and stretched specimens, respectively). $f_c(\lambda)$ was estimated from the wide-angle X-ray diffraction experiments as discussed in detail in the previous paper[1] (the result being shown in *Figure 2*). $\Delta_{\text{assembly}}(\lambda)$ is estimated from equations (4), (5) and (6) if $\epsilon_{c,x}$, $\epsilon_{c,z}$, $\epsilon_{a,x}$, $\epsilon_{a,z}$, and ϕ_c are all known as a function of λ. If only the thickness of amorphous layer l changes with λ but the thickness of crystalline layer (lamella) 'a' remains constant, then:

$$\phi_c(\lambda) = a/L = (a/L_0)(L_0/L) = \phi_{c,0}/\lambda \tag{10}$$

since the bulk elongation ratio is identical to the elongation ratio of the interlamellar spacing, where $\phi_{c,0}$ is the volume-

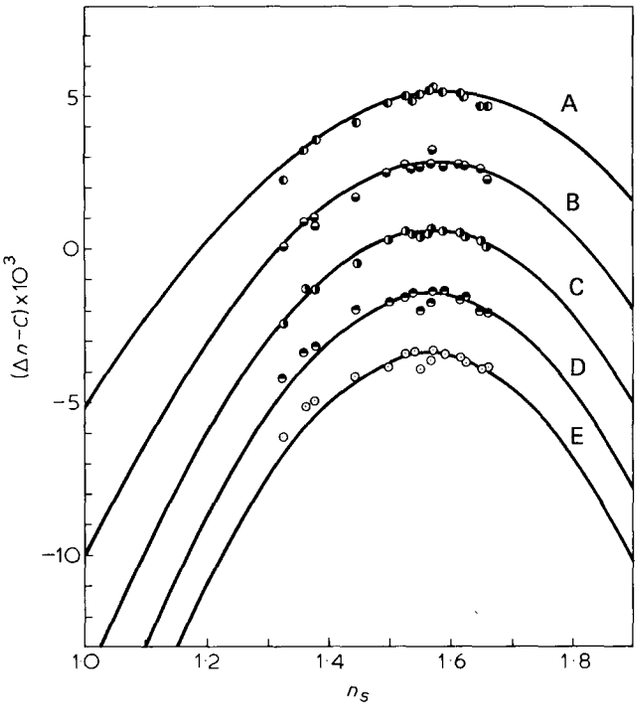

Figure 3 Variation of the birefringence Δn for the specimens stretched by the various extension ratios λ with refractive indices of the immersion liquids as shown in *Table 1*. The points and full lines correspond to the measured and calculated Δn. The calculated values were obtained for $\Delta_c^0 = 0.0108$, $n_{c,z} = 1.544$ and $n_{a,z}^0 = 1.505$; ——, theoretical curve

Symbol	λ	c
A	1.295	0
B	1.390	2
C	1.485	4
D	1.580	6
E	1.650	8

average crystallinity for the undeformed specimen which was measured by wide-angle X-ray diffraction and differential scanning calorimetry. *Figure 2* also shows ϕ_c as a function of λ.

It is assumed that $\epsilon_{c,x}$ and $\epsilon_{c,z}$ are independent of λ but $\epsilon_{a,x}$ and $\epsilon_{a,z}$ vary with λ because of the density lowering of the interlamellar amorphous region. As discussed in the previous paper, there should exist a large number of tie chains in the amorphous region. Therefore the extensions of the amorphous layers are assumed to result in a lowering of density of the amorphous phase. We shall consider the variations of $\epsilon_{a,x}$ and $\epsilon_{a,z}$ with elongation and immersion in liquids immediately in the next section.

Suppose that molecules 1 and 2, each having dielectric constant ϵ_1 and ϵ_2, form a *uniform mixture*, then the dielectric constant of the mixture $\langle\epsilon\rangle$ may be given by:

$$\langle\epsilon\rangle = \epsilon_1\phi_1 + \epsilon_2\phi_2; \phi_1 + \phi_2 = 1 \tag{11}$$

where ϕ_1 and ϕ_2 are the volume fractions of the components 1 and 2, respectively.

When a load is applied parallel to the axis of the lamellar assembly, then the interlamellar spacing increases and thus the interlamellar amorphous layer thickens from l_0 to l. The deformation involves a uniform lowering of the density of the amorphous phase and orientation of the tie chains, thus the dielectric constants being changed from $\epsilon_{a,z}^0$ and $\epsilon_{a,x}^0$ for undeformed state to $\epsilon_{a,z}(\lambda)$ and $\epsilon_{a,x}(\lambda)$ (λ is the elongation ratio of the interlamellar spacing). The decrease of the dielectric constants due to the density lowering of the interlamellar amorphous region may be described in principle using equation (11), i.e. uniform mixing of the air molecules having the dielectric constant ϵ_v and the volume fraction ϕ_v with amorphous materials having the dielectric constants $\epsilon_{a,z}^0$ and $\epsilon_{a,x}^0$ and the volume fraction $(1-\phi_v)$.

Therefore

$$\epsilon_{a,z}(\lambda) = \epsilon_{a,z}^0(1-\phi_v) + \epsilon_v\phi_v \tag{12}$$

$$\epsilon_{a,x}(\lambda) = \epsilon_{a,x}^0(1-\phi_v) + \epsilon_v\phi_v \tag{13}$$

The volume fraction ϕ_v is estimated from the extensions of the amorphous layer:

$$\phi_v(\lambda) = (l-l_0)/l = (\lambda-1)/(\lambda-\phi_{c,0}) \tag{14}$$

where l_0 and l are the thicknesses of the amorphous layer for the undeformed and deformed specimens, respectively (*Figure 1*). The orientation of amorphous chains also contributes to $\epsilon_{a,z}(\lambda)$ and $\epsilon_{a,x}(\lambda)$ and adds an additional term in right hand side of equations (12) and (13). This contribution to the absolute values of $\epsilon_{a,z}(\lambda)$ and $\epsilon_{a,x}(\lambda)$ [not to the difference between $\epsilon_{a,z}(\lambda)$ and $\epsilon_{a,x}(\lambda)$] is supposed to be small and thus neglected in this analysis.

In the case when the stretched specimens are immersed in a liquid of dielectric constant ϵ_s, the liquid interpenetrates the interlamellar amorphous phase and simply replaces air molecules. If this is the case, then the dielectric constants $\epsilon'_{a,z}(\lambda)$ and $\epsilon'_{a,x}(\lambda)$ may be given by:

$$\epsilon'_{a,z}(\lambda) = \epsilon_{a,z}^0(1-\phi_v) + \epsilon_s\phi_v \tag{15}$$

$$\epsilon'_{a,x}(\lambda) = \epsilon_{a,x}^0(1-\phi_v) + \epsilon_s\phi_v \tag{16}$$

where it is assumed that the liquid is inert to the specimens except that it replaces the air phase. The assumption may be poor at small elongations but good at large elongations. The dielectric constants of the crystalline phases are assumed to be independent of λ and immersion liquids:

$$\epsilon'_{c,z}(\lambda) = \epsilon_{c,z}(\lambda) = \epsilon_{c,z} = n_{c,z}^2 \tag{17}$$

$$\epsilon'_{c,x}(\lambda) = \epsilon_{c,x}(\lambda) = \epsilon_{c,x} = n_{c,x}^2 \tag{18}$$

METHODS OF EVALUATING THE PARAMETERS

When a specimen stretched to a given elongation is immersed in a liquid of refractive index n_s [$=(\epsilon_s)^{1/2}$] liquid replaces air and increases the refractive index of the amorphous layer from $\epsilon_{a,z}(\lambda)$ and $\epsilon_{a,x}(\lambda)$ to $\epsilon'_{a,z}(\lambda)$ and $\epsilon'_{a,x}(\lambda)$. This results in a decreased contribution of the form birefringence which is negative in sign, since the lamellae are oriented normal to the *ED*. Thus the liquids tend to increase the net birefringence Δn for a given λ as shown in *Figure 3* where the variation of observed (points) and calculated (full lines) Δn with n_s are shown for various extension ratios λ, and C is the scale factor to avoid an overlap of each data points. The calculated results will be discussed in next section. The maximum value of the birefringence Δn^* is attained when the refractive index of the amorphous phase becomes identical to that of the crystalline phase, ie.. when the contribu-

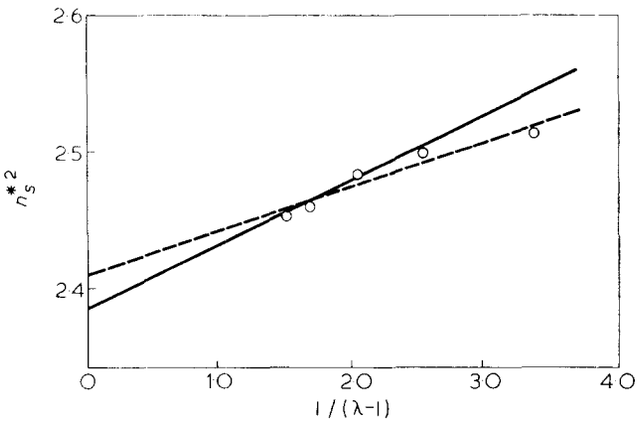

Figure 4 Plots of n_s^{*2} vs. $(\lambda - 1)^{-1}$ based upon equation (23). The broken and full lines give a set of values $n_{c,z} = 1.551$, $n^{\circ}_{a,z} = 1.524$ and $n_{c,z} = 1.545$, $n^{\circ}_{a,z} = 1.505$, respectively.

tion of the form birefringence becomes a minimum.

Let the refractive index of the liquid at which the contribution of the form birefringence becomes a minimum and therefore Δn becomes maximum be $n_s^* = (\epsilon_s^*)^{1/2}$. The measurable quantities n_s^*, Δn^* and the shape of the entire curve of Δn with n_s can be explained in terms of the characteristic parameters of the system and reduce the number of unknown parameters as described below.

It follows that at $\epsilon_s = \epsilon_s^* = n_s^{*2}$ the birefringence Δn becomes maximum, and therefore from equations (6) and (8):

$$\partial \Delta n/\partial \epsilon_s = f_z \partial \Delta_{\text{assembly}}/\partial \epsilon_s = f_z \partial(\epsilon_z^{1/2} - \epsilon_x^{1/2})/\partial \epsilon_s = 0 \tag{19}$$

The dielectric constants of the assembly ϵ_z and ϵ_x are given by equations (4) and (5) where $\epsilon_{c,x}$, $\epsilon_{c,z}$, $\epsilon_{a,x}$ and $\epsilon_{a,z}$ should be replaced by $\epsilon'_{c,x}(\lambda)$, $\epsilon'_{c,z}(\lambda)$, $\epsilon'_{a,x}(\lambda)$ and $\epsilon'_{a,z}(\lambda)$ given by equations (15) and (18).

Noticing that:

$$\epsilon'_{c,x}(\lambda) \simeq \epsilon'_{c,z}(\lambda); \epsilon'_{a,x}(\lambda) \simeq \epsilon'_{a,z}(\lambda) \tag{20}$$

and the relation followed by equations (15) and (16):

$$\partial \epsilon'_{a,z}(\lambda)/\partial \epsilon_s = \partial \epsilon'_{a,x}(\lambda)/\partial \epsilon_s = \phi_v(\lambda) \tag{21}$$

we obtain:

$$\epsilon'_{c,z}(\lambda) = \epsilon'_{a,z}(\lambda) \tag{22}$$

From equations (15), (17), and (22):

$$\epsilon_{c,z} = \epsilon^0_{a,z}(1 - \phi_v) + \epsilon_s^* \phi_v$$

and using equation (14), the equation is rewritten as:

$$(n_s^*)^2 = (1 - \phi_{c,0})(n_{c,z}^2 - n_{a,z}^{02})/(\lambda - 1) + n_{c,z}^2 \tag{23}$$

The equation explains the decrease of the value of n_s^* with increasing λ as in *Figure 3*. Therefore, a plot of the type shown in *Figure 4* gives unknown parameters $n_{c,z} = \epsilon_{c,z}^{1/2}$ and $n^0_{a,z} = (\epsilon^0_{a,z})^{1/2}$.

For $n_s = n_s^*$ where equation (22) is valid, it can be shown that:

$$\Delta^*_{\text{assembly}} \equiv \Delta_{\text{assembly}}(n = n_s)$$
$$\simeq \phi_c \Delta^0_c + (1 - \phi_c)\Delta^0_{\text{amp}} \tag{24}$$

In this case, therefore, the additivity of the birefringence is established. The equation explains the dependence of the maximum birefringence Δn^* with λ in *Figure 3*.

From equations (8)–(10) and (24), $\Delta n^* = \Delta n(n = n_s)$ of the system is given by:

$$\frac{\Delta n^*}{f_c} = \frac{\phi_{c,0}}{\lambda}\Delta^0_c + \left(1 - \frac{\phi_{c,0}}{\lambda}\right)\Delta^0_{\text{amp}}(\lambda) \tag{25}$$

where $\Delta n^*/f_c$ can be measured as a function of λ, and a relative variation of $(\Delta n^*/f_c)\lambda$ with λ is purely associated with that attributed to the amorphous phase (see *Figure 5*).

Thus if $\Delta^0_c (= \epsilon_{c,z}^{1/2} - \epsilon_{c,x}^{1/2})$ is known, we can estimate $\Delta^0_{\text{amp}}(\lambda) = f^0_{\text{am}}(\lambda)\,\Delta^0_{\text{amc}} = [\epsilon_{a,z}(\lambda)]^{1/2} - [\epsilon_{a,x}(\lambda)]^{1/2}$, i.e. the birefringence of the amorphous layer in dry and stretched conditions. The quantity f^0_{am} is the second order orientation factor of the amorphous chain segments with respect to the assembly axis z. Since a plot of the type shown in *Figure 4* yields the values for $\epsilon_{c,z}$ and $\epsilon^0_{a,z}$ we can estimate all the necessary parameters, $\epsilon_{c,x}$, $\epsilon_{c,z}$, $\epsilon^0_{a,x}$, and $\epsilon^0_{a,z}$ [or $\epsilon_{a,x}(\lambda)$, $\epsilon_{a,z}(\lambda)$, $\epsilon_{a,x}'(\lambda)$, and $\epsilon'_{a,z}(\lambda)$] to calculate the birefringence of the assembly Δ_{assembly}, net birefringence of the system Δn, apparent form birefringence of the assembly Δ^0_{form} and from that system Δ_{form}:

$$\Delta_{\text{form}} = f_z \Delta^0_{\text{form}} = f_z(\Delta_{\text{assembly}} - \Delta^*_{\text{assembly}})$$
$$= \Delta n - f_z(\phi_c \Delta^0_c + \phi_a \Delta^0_{\text{amp}}) \tag{26}$$

Other parameters $n_s = \epsilon_s^2$, $\lambda = L/L_0$, $\phi_{c,0}$ and f_c are all measurable.

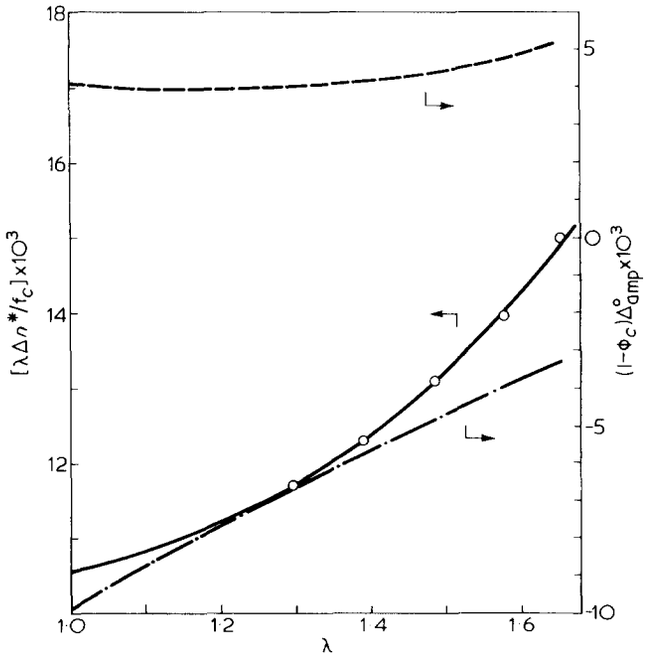

Figure 5 Plots of $(\Delta n^*/f_c)\lambda$ and of $(1 - \phi_c)\,\Delta^{\circ}_{\text{amp}}(\lambda)$ (the birefringence of the amorphous layer in the one-dimensional assembly shown in *Figure 1*) as a function of λ based upon equation (25). In the plot of $(1 - \phi_c)\Delta^{\circ}_{\text{amp}}(\lambda)$ vs. λ, Δ°_c was assumed to be 0.0108 for the broken line and 0.0340 for the dash-dot line.

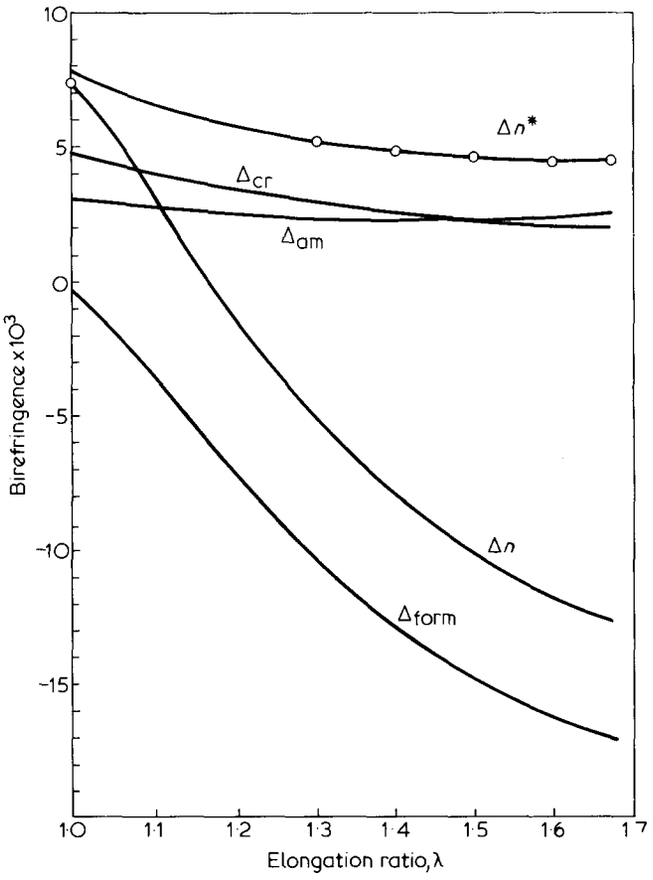

Figure 6 Plots of the measured Δn^* and of estimated result of Δn and its separation into Δ_{form}, Δ_{cr} and Δ_{am} for $\Delta_c^0 = 0.0108$, $n_{c,z} = 1.544$ and $n_{a,z}^0 = 1.505$

RESULTS AND DISCUSSIONS

Figure 2 represents the variation of the orientation factor f_c for the crystal *c*-axis with the applied extension of the specimen λ. The factor f_c was measured as described in the previous paper[1] and was assumed to be equal to f_z, the orientation factor of the assembly axis *z* (*Figure 1*). The variation of the volume-average crystallinity $\phi_c = \phi_{c,0}/\lambda$ (equation 10) was estimated from equality of the bulk extension ratios and the extension ratios of the lamellar spacings as clarified by the small-angle X-ray scattering studies[1]. Although $\phi_{c,0}$ measured from d.s.c. and wide-angle X-ray diffraction studies was 0.60 and 0.55, respectively, the value of 0.6 was used in the following analyses. The Figure also includes the parameter associated with the extension of the thickness in the amorphous layer. $\phi_v = (l - l_0)/l = (\lambda - 1)/(\lambda - \phi_{c,0})$ (equation 14). These parameters $f_c(\lambda)$, $\phi_c(\lambda)$ and $\phi_v(\lambda)$ were used in the following analyses.

Figure 3 represents the variations of the net birefringence of the specimens Δn with refractive indices of the immersion liquids shown in *Table 1* for the specimens stretched by the various extension ratios λ. From the Figure one can measure the parameters n_s^* and Δn^* (as discussed in the previous section) as a function of λ which can be used for further analyses of the types as shown in *Figures 4* and *5*.

The birefringence Δn for a given λ becomes a maximum (Δn^*) for $n = n_s^*$, since the negative values of Δ_{form} becomes a minimum in this condition. Therefore the values of Δn^* as a function of λ (as plotted in *Figure 6*) give the variation of birefringence arising from the molecular orientation in the crystalline and amorphous phases with λ. It should be noted that the value of n_s^* is greater than the average refractive index of the amorphous and crystalline phases (nearly equal to 1.52 and 1.55, respectively, as discussed immediately below). This is because the liquid which penetrates into the amorphous phase should increase the refractive index of the amorphous phase up to that of the crystalline phase in order to minimize the contribution Δ_{form}.

Figure 4 represents the plots of (n_s^{*2}) vs. $(\lambda - 1)^{-1}$, which gives the values of $n_{c,z} = 1.551$ and $n_{a,z}^0 = 1.524$ (broken line) and $n_{c,z} = 1.544$ and $n_{a,z}^0 = 1.505$ (full line) based upon equation (23). The former set of values obtained from the broken line seems to be more reasonable than the latter set of values. It is clear that the greater the value of λ, the smaller is the value of n_s^*. This is reasonable since the volume occupied by the liquids ϕ_v increases with increasing λ.

Figure 5 shows plots of $(\Delta n^*/f_c)\lambda$ and of $(1 - \phi_c)\Delta_{amp}^0(\lambda) = (1 - \phi_c)[(\Delta n^*/f_c)\lambda - \phi_{c,0}\Delta_c^0]/(\lambda - \phi_{c,0})$, i.e. the birefringence of the amorphous layer in dry state and in the one-dimensional assembly (as shown in *Figure 1*) as a function of λ. These plots are based upon equation (25). If Δ_c^0 is known, then one can estimate $\Delta_{amp}^0(\lambda) = \epsilon_{a,z}(\lambda)^{1/2} - \epsilon_{a,x}(\lambda)^{1/2} = n_{a,z}(\lambda) - n_{a,x}(\lambda)$ as a function of λ from the plot of $\lambda(\Delta n^*/f_c)$ vs. λ. The results on $(1 - \phi_c)\Delta_{amp}^0(\lambda)$ are plotted by broken (for $\Delta_c^0 = 0.0108$)[12] and dash-dot (for 0.0340)[13] lines. The increase of $(1 - \phi_c)\Delta_{amp}^0(\lambda)$ with λ should be interpreted in terms of variation of $(1 - \phi_c)$ and of f_{am}^0, the second-order orientation factor for the amorphous chain in the assembly, since

$$\Delta_{amp}^0(\lambda) = f_{am}^0 \Delta_{amc}^0 \tag{27}$$

It should be noted that f_{am} in equation (1), the orientation factor of the amorphous chain with respect to the extrusion direction, is related to f_{am}^0 and $f_z (\simeq f_c)$ by $f_{am} = f_{am}^0 f_z$. The factor f_{am}^0 should increase due to orientation of the tie chain accompanied by the increase of the thickness l of the amorphous layer, and $(1 - \phi_c)$ should also increase with λ (*Figure 2*).

Therefore, if Δ_c^0 is known, then all the parameters $\epsilon_{c,x}(\lambda)$, $\epsilon_{c,z}(\lambda)$, $\epsilon_{a,x}(\lambda)$, and $\epsilon_{a,z}(\lambda)$ or the corresponding quantities in the immersion liquids $\epsilon_{c,x}'(\lambda)$ etc. can be estimated, and therefore Δn, $\Delta_{assembly}$, Δ_{form}, and Δ_{form}^0 can be estimated in dry and immersed states as a function of λ.

It should be noted that the estimated birefringence of the assembly arising from the amorphous chain orientation $(1 - \phi_c)\Delta_{amp}^0$ strongly depends upon the $\Delta^0{}_c$, intrinsic birefringence of the crystal in the stable modification. With the value $\Delta_c^0 = 0.034$ obtained experimentally by Tanaka *et al.*[13], it becomes negative as shown in *Figure 5* for the whole range of λ. In the light of the deformation and orientation mechanisms already discussed in this and previous papers, i.e., the orientation of amorphous chain segments accompanied by the extension of the interlamellar spacing, it seems to be difficult to explain the negative orientation of the amorphous chain segments. This negative birefringence may be attributed to an overestimation of Δ_c^0. The relative variation of the birefringence with λ, however, seems to be capable of being described in terms of the deformation mechanism; with increasing λ the thickness of the amorphous layers, l, increases and thus f_{am}^0 and $(1 - \phi_c)$ increase to result in the increasing $(1 - \phi_c)\Delta_{amp}^0$. With the theoretical value of $\Delta_c^0 = 0.0108$ by Stein *et al.*[12] the birefringence $(1 - \phi_c)\Delta_{amp}^0$ are all positive for whole range of λ and increase slightly with λ, the tendency of which may be qualitatively explained by the orientation mechanism. For quantitative analyses of the amorphous chain orientation on the

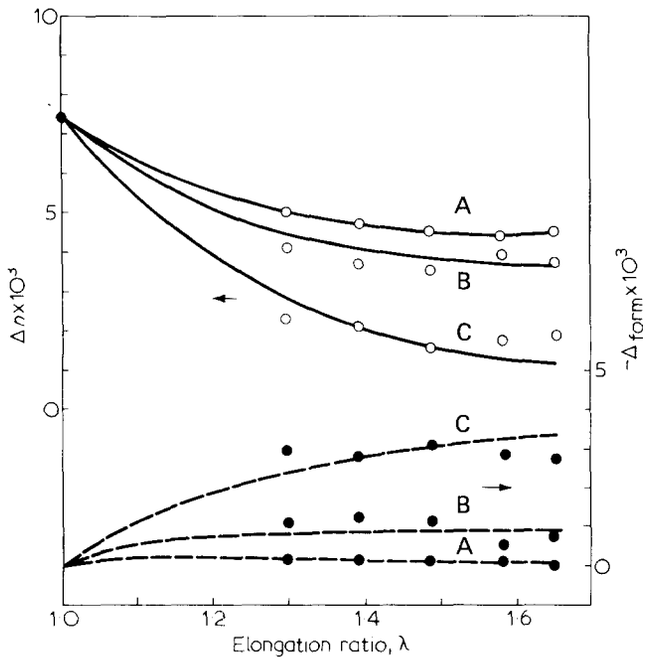

Figure 7 Comparisons between the calculated Δn (full lines) and Δ_{form} (broken lines) with the measured Δn (○) and Δ_{form} (●) for the specimens stretched and immersed in liquids. The calculated results were obtained for the same set of parameters as in *Figure 6*. Curves (A), (B), (C) correspond to those obtained by immersing the stretched specimens in chlorobenzene, chloroform and methanol, respectively

basis of simulating the experimental results of the models employed by Stein *et al.*[6] and Gaylord *et al.*[7] it is essential to evaluate rigorously the value of Δ_c^0.

Figure 6 represents the estimated result on Δn for $\Delta_c^0 = 0.0108$, and its resolution into each contribution; $\Delta n^* = \Delta_{cr} + \Delta_{am}$, $\Delta_{cr} = f_c \phi_c \Delta_c^0$ and $\Delta_{am} = (1 - \phi_c) f_{am} \Delta_{amc}^0 = f_c(1 - \phi_c)\Delta_{amp}^0$ and $\Delta_{form} = f_c \Delta_{form}^0$. The values of Δn and Δ_{form} are estimated for dry specimens. The values of Δn^* were measured from the type of experiments as shown in *Figure 3*, which were then separated into crystalline and amorphous contributions, i.e., Δ_{cr} and Δ_{am}, respectively, based upon equation (25), measured quantities $f_c(\lambda)$ and $\phi_c(\lambda)$ and assumed value of $\Delta_c^0 = 0.0108$. The values for Δn were estimated based upon the Franklin's theory by using the estimated refractive indices. These values for Δn cannot be directly compared with the experimental results, since the specimens become opaque with stretching so that they cannot be measured under dry state.

The apparent form birefringence Δ_{form} which is obtained by $(\Delta n - \Delta n^*)$ is small ($\sim -5 \times 10^{-4}$) compared with Δn^* ($\sim 7.5 \times 10^{-3}$) related to crystal and amorphous chain orientations for the undeformed state. However, the negative value of Δ_{form} increases with increasing λ and becomes comparable to Δn^* at $\lambda \simeq 1.15$, giving rise to a value of Δn nearly equal to zero. With a further increase of λ, Δ_{form} dominates over the Δn^* so that Δn exhibits large negative values. Thus it is clear that the relative variation of Δn with λ is primarily determined by that of Δ_{form} and that one cannot estimate the birefringence arising from the molecular orientation without subtracting the Δ_{form} for such a stacked lamellar system.

It is important to note that that the variation of Δ_{am} with λ is different to that of Δ_{cr} with λ. If the (regular and loose) loops and the cilia are the major fraction of the amorphous materials, then the variation of Δ_{am} with λ may be similar to that of Δ_{cr} with λ, since the segments of these amorphous components should orient in a similar way to the orientation of the axes normal to the basal plane of lamellae, i.e., in a similar way to the crystal c-axis. The difference of the behaviours of Δ_{am} and Δ_{cr} with λ, or, more quantitatively, $\Delta_{am}/(1 - \phi_c)$ and Δ_{cr}/ϕ_c with λ may suggests a substantial contribution of orientation of the tie chains. Further quantitative analyses of the amorphous chain orientations would require some model calculations of the type as proposed by Stein *et al.*[6] and Gaylord *et al.*[7], though this is beyond the scope of the present article. It is also noted that the variations of Δ_{am} and Δ_{cr} with λ strongly depend upon Δ_c^0. Therefore the quantitative analyses would require rigorous determination of Δ_c^0. The values for Δ_{cr} decrease with increasing λ, which is primarily associated with decreasing f_c as shown in *Figure 2* due to deformation of the sheaf-like superstructure and orientation of the lamellar axis toward the stretching direction (i.e., disorientation of the assembly z-axis with the stretching direction). The variation of Δ_{am} with λ is relatively small compared with that of Δ_{cr}, because the increase of the birefringence of the amorphous layer $(1 - \phi_c)\Delta_{amp}^0$ in the assembly (see *Figure 5*) tends to be compensated by the disorientation of the assembly, i.e. by the decrease of $f_c(\Delta_{am} = f_c(1 - \phi_c)\Delta_{amp}^0)$

The solid lines in *Figure 3* show the values for Δn for stretched and immersed specimens which are evaluated based upon the estimated parameters as described above. Again Δ_c^0 is assumed to be 0.0108 and a set of values $n_{c,z} = 1.544$ and $n_{a,z}^0 = 1.505$ is used. A fine agreement between the calculated and measured values was obtained. *Figure 7* represents similar comparisons of the calculated total birefringence Δn and form birefringence Δ_{form} with the respective measured birefringences. The measured form birefringence (●) was estimated from the measured total birefringence Δn (○) by using a relationship $\Delta_{form} = \Delta n - \Delta n^*$ and was compared with the calculated Δ_{form} (broken lines). The calculated results were obtained for the same set of parameters as in *Figure 6*. Again relatively good agreements between the calculated and measured Δ_{form} and Δn are obtained, which supports the validity of the deformation models involving the lamellar orientation and a uniform density lowering in the interlamellar amorphous regions caused by the extension of the interlamellar spacing.

The fact that Δ_{am} is approximately equal to Δ_{cr} and, more directly, the qualitative indication of substantial contribution of amorphous tie chains to Δ_{am} are consistent with the model proposed in the previous paper (*Figure 10d* in Part I) on the deformation behaviour of lamellar and amorphous regions in order to explain the springy properties observed at temperatures above the glass transition. At temperatures above the glass transition temperatures, the tie chains are capable of being oriented accompanied by the extensions of the interlamellar amorphous regions. The orientation of the tie chains and the lamellar bending between the tie links or chains can be an origin of the retractive force of the long range elasticity. However, at temperatures below the glass transition temperatures, where the micro-Brownian motion of chain molecules are frozen, deformation of the amorphous phase does not involve orientation of the tie chains but involves intermolecular deformation, bond stretching and bending of the valence angles which are not able to undergo the large recoverable deformation.

The results obtained in this article are also important in understanding dynamic birefringence of the films. *Figure 8* represents the frequency dependencies of the real $K'(\omega)(a)$ and imaginary $K''(\omega)(b)$ parts of the strain–optical coeffi-

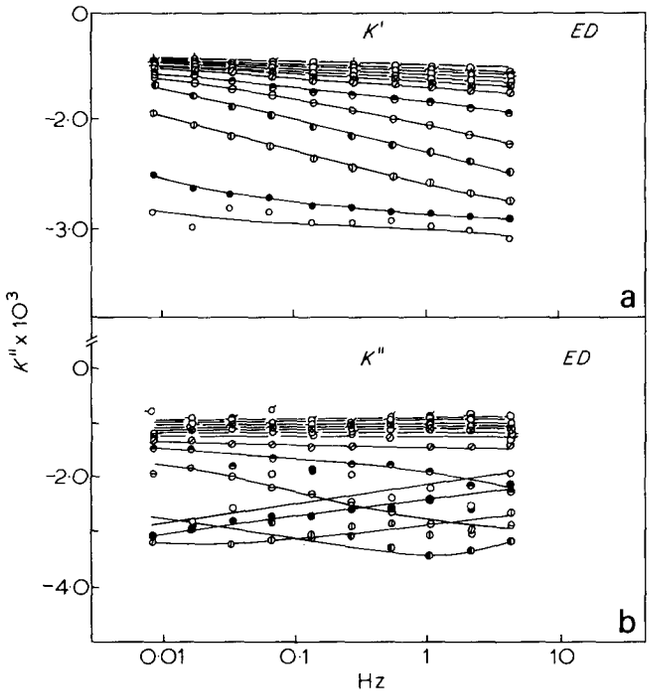

Figure 8 Frequency dependencies of (a) the real ($K'(\omega)$) and (b) imaginary [$K''(\omega)$] parts of the strain–optical coefficients ($\partial\Delta n/\partial\epsilon$) at various temperatures in linear viscoelastic range (static and dynamic strain being 3 and 0.3%, respectively). Excitation along the *ED*. ○, −50°C; ●, −40; ⊕, −30; ◐, −20; ⊖, −10; ◓, 0; ⊘, 10; ⊗, 20; ○, 30; ○, 40; ○, 52; ♂, 60; ♀, 69; ♁, 78

cients $\partial\Delta n/\partial\epsilon$ at various temperatures in linear viscoelastic range (static strain 3% and dynamic strain 0.3%). The data indicate that the time and temperature-dependence of the $K'(\omega)$ and $K''(\omega)$ are small at temperatures above room temperature and that the magnitude of the loss tangent $\tan\delta = K''(\omega)/K'(\omega)$ and thus the phase difference between the dynamic birefringence and strain is small, suggesting an elastic response of the films. The loss tangent becomes maximum at the glass transition temperature owing primarily to the loss mechanisms in the orientational response of amorphous chains and probably crystals too which are caused by onset of the micro-Brownian motion in the amorphous phase. The negative strain–optical coefficients reflect the negative strain–birefringence coefficient as studied in this work. It is clear from the present studies that the negative values of K'' and K'' are determined by a balance of the time-dependent orientation and deformation processes which give rise to negative dynamic birefringence; the lamellar orientation and the form birefringence associated with the extensions of the interlamellar amorphous regions, and that which gives rise to positive dynamic birefringence; the orientation of the amorphous tie chains. Such studies would be essential to understand the nature of dynamic mechanical dispersions and will be reported elsewhere[14].

ACKNOWLEDGEMENTS

This work was partly supported by a grant through the Japan–US Cooperative Research Program; Japan Society for Promotion of Science and National Science Foundation, USA, to which the authors are deeply indebted. The authors are also indebted to the Mitsui Petrochemical Industries, Ltd, Tokyo, Japan, for financial support through a scientific grant.

REFERENCES

1 Hashimoto, T., Todo, A., Tsukahara, Y., and Kawai, H. *Polymer* 1979, **20**, 636
2 Sprague, B. S. *J. Macromol. Sci. (B)* 1973, **8**, 157
3 Cannon, S. L., McKenna, G. B. and Statton, W. O. *J. Polym. Sci. (Macromol. Rev.)* 1976, **11**, 209
4 Quynn, R. G. and Brody, H. *J. Macromol. Sci. (B)* 1971, **5**, 721
5 Wiener, O. *Abh. Sachs. Akad. D. Wiss, Math. Phys. (K1)* 1912, **32**, 507
6 Petraccone, V., Sanchez, I. C. and Stein, R. S. *J. Polym. Sci., (Polym. Phys. Edn)* 1975, **13**, 1991
7 Lohse, D. J. and Gaylord, R. J. *Polym. Eng. Sci.* 1978, **18**, 512
8 Tsukahara, Y., Hashimoto, T. and Kawai, H. in preparation
9 Cvikl, B., Moroi, D. and Franklin, W. *Mol. Cryst. Liquid Crystl.* 1971, **12**, 267
10 Hashimoto, T., Todo, A., Hashimoto, K. and Kawai, H. *Rep. Prog. Polym. Phys. Jpn* 1977, **20**, 461
11 Vonk, C. G. *J. Appl. Crystallogr.* 1973, **6**, 81
12 Stein, R. S., Keedy, D. A., Powers, J. and Plaza, A. *J, Polym. Sci.* 1962, **62**, S89
13 Tanaka, A., Sugimoto, N., Asada, T. and Onogi, S. *Polym. J.* 1975, **7**, 529
14 Tsukahara, Y., Hashimoto, T. and Kawai, H. in preparation